Physica B: Condensed Matter 560 (2019) 103–110

Contents lists available at ScienceDirect

Physica B: Condensed Matter

journal homepage: www.elsevier.com/locate/physb

Growth and characterization of spray deposited quaternary Cu_2FeSnS_4 semiconductor thin films

Santosh G. Nilange, Nandkishor M. Patil, Abhijit A. Yadav*

Thin Film Physics Laboratory, Department of Physics, Electronics and Photonics, Rajarshi Shahu Mahavidyalaya, (Autonomous), Latur, 413512, Maharashtra, India

ARTICLE INFO

Keywords:
Spray pyrolysis
X-ray diffraction
Semiconducting materials
Optical properties
Electrical properties

ABSTRACT

Quaternary stannite Cu_2FeSnS_4 thin films (CFTS) have been grown on well cleaned amorphous glass substrates at various deposition temperatures (175 °C–325 °C) by chemical spray pyrolysis. CFTS thin films have been characterized to examine the structural, morphological, compositional, optical and electrical properties. Tetragonal crystal structure has been confirmed from X-ray diffraction. Crystalline size was found to be 10–18 nm. Scanning electron microscopy showed monodisperse particles with hexagonal morphologies. Energy dispersive analysis by X-rays study confirmed stoichiometric deposition of CFTS thin films. The direct bandgap was found to be 1.54 eV for CFTS thin film deposited at 250 °C. It was observed that film resistivity drop at deposition temperature of 250 °C. The structural, morphological, compositional, optical and electrical properties of CFTS films have been found to be deposition temperature dependent. An appropriate optical band gap of 1.54 eV and a noteworthy and stable electrical property indicate their prospective for solar cell applications.

1. Introduction

Presently, severe energy crisis and the environmental pollution have forced researchers to advance clean energy resources as an alternative to the fossil fuels. Renewable energy sources including hydro, wind, geothermal, solar and tidal are unlimited, pollution free and environmental friendly [1–3]. Amongst these sources, solar is the best alternative to meet the rising energy demands of the modern society. The resurgence of interest in photovoltaics has stimulated research on new materials and approaches for the fabrication of inexpensive thin film solar cells [4,5].

Several renowned materials including $Cu(InGa)Se_2$ (CIGS) [6], $Cu_2ZnSn(Se,S)_4$ (CZTS) [7], Cu_2FeSnS_4 (CFTS) [8], CdTe [9], TiO_2 [10] have been broadly studied for thin film solar cells. CIGS based solar cells have revealed impressive photo conversion efficiency [11]. But, because of its expensive and scarce elements like indium and gallium, CIGS solar cells cannot be used extensively. To achieve the goal of cost effective photovoltaic technology, it is necessary to explore other semiconducting materials containing less toxic sulphur instead of selenium and more abundant iron than indium for CFTS. Stannite CFTS is considered to be one of the most eligible photovoltaic materials due to the abundant and nontoxic constituents, high absorption coefficient ($10^{-4}\,cm^{-1}$) and suitable bandgap (1.2–1.5 eV) for solar cell applications [8,12].

Vanalakar et al. [13] has provided a review on CFTS thin films for solar cell applications. The same group has developed a simple, low cost and industrial scalable ball milling procedure for the eco-friendly synthesis of CFTS powder [14]. They confirmed pure CFTS phase through XRD, Raman spectroscopy and EDX analysis with a band gap of 1.42 eV. Fidha and colleagues [15] deposited tetragonal quaternary CFTS films onto glass substrates at 370 °C for one hour with post-sulfurization treatment at 450 °C for 30 min. Raman spectrum confirmed appearance of two main peaks corresponding to the CFTS situated at the positions 289 cm^{-1} and 318 cm^{-1}. Wang and coworkers [8] synthesized CFTS thin films via a convenient blade-coating technique. It have been witnessed that the addition of Rb ions in CFTS improves the grain size and surface morphology. Meng and coworkers [16] studied the effect of holding times of sulfurization on the morphological properties of CFTS films. SEM images showed that films have smooth, closely packed and no voids surface. They concluded that the longer holding time was in favor of the grain growth. Zhang et al. [17] have synthesized oblate spheroid and triangular plate shape CFTS nanocrystals with band gap of 1.54 ± 0.04 eV and 1.46 ± 0.03 eV respectively using solution based method.

Guan and colleagues [18] have prepared CFTS films through successive ionic layer absorption and reaction combined with chemical bath deposition. The measurements showed large agglomeration of rod-shaped CFTS grains, with bandgap of 1.22 eV and absorption coefficient of > $10^4\,cm^{-1}$. Dong and colleagues [19] have prepared CFTS nanoparticles on FTO substrates by spin coating. The CFTS film had a band gap of 1.53 eV and an absorption coefficient higher than

* Corresponding author.
E-mail address: aay_physics@yahoo.co.in (A.A. Yadav).

https://doi.org/10.1016/j.physb.2019.02.008
Received 18 January 2019; Received in revised form 3 February 2019; Accepted 4 February 2019
Available online 08 February 2019
0921-4526/

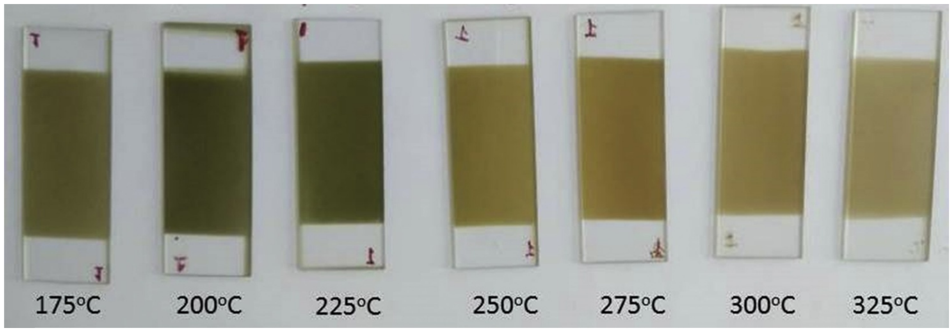

Fig. 1. Photograph of CFTS thin films spray deposited at various deposition temperatures.

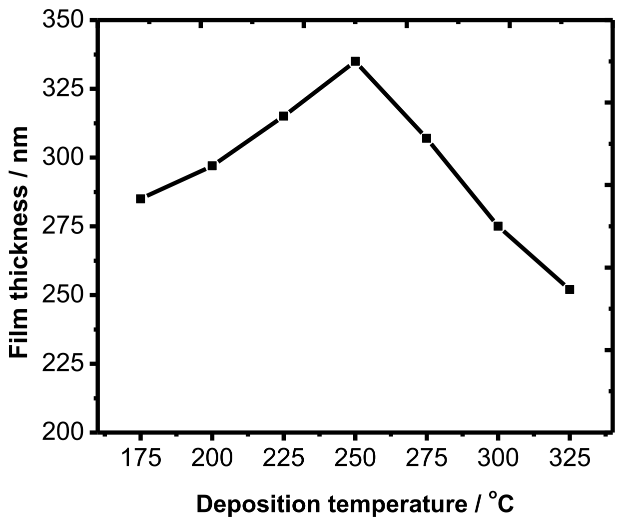

Fig. 2. Variation of film thickness with deposition temperature for spray deposited CFTS thin films.

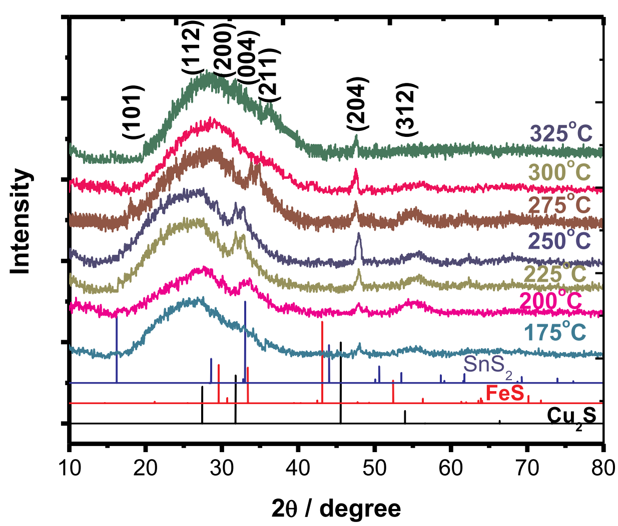

Fig. 3. XRD pattern of CFTS thin films spray deposited at various deposition temperatures (The major peaks of possible impurities Cu_2S, FeS and SnS_2 are included at the bottom).

$10^4\,cm^{-1}$. Jiang and coworkers [20] synthesized tetragonal CFTS nanoparticles with high crystallinity using solvothermal method. Mokurala et al. [21] have synthesized single phase CZTS and CFTS by thermal decomposition. The morphology displayed equiaxed nanoparticles of approximately 10–20 nm and 8–15 nm size, respectively. The optical bandgaps are found to be 1.48 eV and 1.40 eV respectively for CZTS and CFTS.

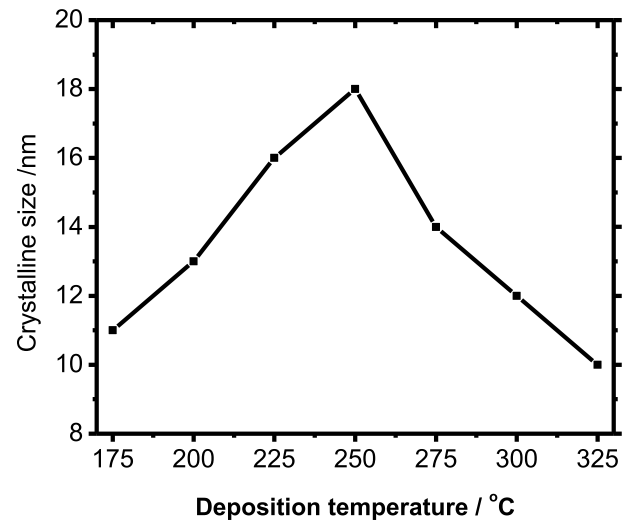

Fig. 4. Variation of crystalline size with deposition temperature for spray deposited CFTS thin films.

Ozel and colleagues [22] have fabricated tetragonal CFTS nanocrystalline fibers with diameters of 100 ± 50 nm through electrospinning technique. Prabhakar and coworkers [23] produced spray deposited p-type CFTS. The CFTS based dye-sensitized solar cell revealed an efficiency of 8.03%. Khadka et al. [24] explored properties of spray deposited Cu_2FeSnX_4 (X: S, Se) thin films. Yan et al. [25] synthesized tetragonal CFTS nanocrystals by a simple hot-injection method. Meng et al. [26] fabricated two Cu based selenide semiconductors using radio-frequency magnetron sputtering. The literature survey shows that various techniques are available to prepare CFTS. However, the methods for synthesizing CFTS are usually complex and time consuming. Keeping in view all these aspects an effort has been made to deposit CFTS thin films at various deposition temperatures and additionally its influence on various properties have been studied. In the course study, it is found that the spray deposited quaternary stannite CFTS thin films have most suitable absorption coefficient and optical bandgap for a thin film solar cell.

2. Experimental

CFTS thin films were deposited on properly cleaned amorphous glass substrates by chemical spray pyrolysis method discussed elsewhere [27]. The equimolar (0.025 M) solutions of $Cu(NO_3)_2{\cdot}3H_2O$, $FeSO_4{\cdot}7H_2O$, $SnCl_4{\cdot}5H_2O$, and CH_4N_2S were prepared in double distilled water. The precursor solution was obtained by mixing above equimolar solutions together in appropriate volumes to have Cu:Fe:Sn:S ratio 2:1:1:4 and then sprayed through a nozzle onto the preheated glass substrates. The deposition temperature was varied from 175 °C to 325 °C at the intervals of 25 °C, by keeping all other parameters constant, especially the molarity of spraying solution (0.025 M). Spray rate employed was 4–5 ml min^{-1} and

Table 1
Structural data of spray deposited CFTS thin films.

Deposition Temperature (°C)	film thickness (nm)	2θ (°)	Observed d(Å)	Standard d(Å)	hkl (Å)	a = b (Å)	c (Å)	D (nm)
175	285	27.99	3.186	3.157	112	5.50	10.65	11
		32.52	2.752	2.725	200			
		33.46	2.677	2.684	004			
		47.71	1.905	1.913	204			
		54.99	1.669	1.641	312			
200	297	27.40	3.254	3.157	112	5.52	10.61	13
		32.40	2.762	2.725	200			
		33.57	2.668	2.684	004			
		38.18	2.356	2.377	211			
		47.59	1.910	1.913	204			
		54.99	1.669	1.641	312			
225	315	27.29	3.266	3.157	112	5.63	10.72	16
		31.73	2.819	2.725	200			
		32.99	2.714	2.684	004			
		47.81	1.901	1.913	204			
		55.54	1.654	1.641	312			
250	335	27.56	3.235	3.157	112	5.63	10.74	18
		31.78	2.814	2.725	200			
		32.66	2.740	2.684	004			
		47.83	1.901	1.913	204			
		55.34	1.659	1.641	312			
275	307	18.20	4.872	4.859	101	5.31	10.51	14
		28.22	3.161	3.157	112			
		33.48	2.675	2.725	200			
		33.71	2.657	2.684	004			
		47.43	1.916	1.913	204			
		55.78	1.647	1.641	312			
300	275	28.07	3.177	3.157	112	5.50	10.72	12
		31.37	2.850	2.725	200			
		38.01	2.366	2.377	211			
		47.43	1.916	1.913	204			
		55.57	1.653	1.641	312			
325	252	27.90	3.196	3.157	112	5.61	10.76	10
		31.84	2.809	2.725	200			
		32.82	2.727	2.684	004			
		39.09	2.303	2.377	211			
		47.50	1.913	1.913	204			
		55.78	1.647	1.641	312			

the nozzle to substrate distance was 30 cm. CFTS films were allowed to cool at room temperature after deposition and it was observed that film adhesion on substrates was quite good.

Thickness of film was determined by using gravimetric weight difference method with sensitive microbalance by assuming bulk density of corresponding materials. Structural characterization of the films was carried out by analysing the XRD patterns obtained through X-ray diffractometer with Cu-Kα radiation (λ = 1.5406 Å), within the 2θ angles between 10° and 80°. Surface morphology and compositional analysis was carried out using JEOL-JSM-6360A microscope. A UV–Vis spectrophotometer (SHIMADZU UV-1700) was used to study optical properties. D.C. two point probe method was used for electrical resistivity measurements. Silver paste was employed to CFTS films to ensure good electrical ohmic contacts.

3. Results and discussion

3.1. Film formation

When a mixed aqueous solution of copper nitrate, ferrous sulfate, stannic chloride and thiourea was sprayed over the preheated glass substrates, a pyrolytic decomposition of solution took place resulting in the formation of well-adherent and uniform CFTS thin films. Photograph of CFTS thin films spray deposited at various deposition temperatures is shown in Fig. 1. The possible reaction mechanism for growth of CFTS thin films can be given as:

$$2Cu(NO_3)_2 3H_2O + FeSO_4 7H_2O + SnCl_4 5H_2O + 4CH_4N_2S \overset{\Delta}{\rightarrow} Cu_2FeSnS_4 + 4NO_2\uparrow + 4CO_2\uparrow + SO_2\uparrow + 4NH_4Cl\uparrow + 4NH_3\uparrow + 12H_2O\uparrow + 2O_2\uparrow \quad (1)$$

Simillar type of reaction has been reported by Chen and colleagues [28] for spray deposited CFTS films. The film thicknesses were determined by simple gravimetric weight difference method using sensitive microbalance [29]. Fig. 2 displays variation of film thickness with deposition temperature for CFTS thin films. It is perceived that the film thicknesses upsurges with rise in deposition temperature from 175 °C to 250 °C, reaches maximum (335 nm) at 250 °C and falls further with rise in deposition temperature above 250 °C. The probable reason for such a behavior is: initially the deposition temperature may be insufficient for decomposition to occur, at 250 °C the decomposition of precursor solution occurs at optimum rate resulting in maximum film thickness for CFTS. Above 250 °C the evaporation of precursor material may shrinkage the CFTS film thicknesses [30].

3.2. Structural studies

Fig. 3 shows typical XRD pattern of CFTS thin films spray deposited at various deposition temperatures. XRD analysis revealed that the CFTS films are polycrystalline. The comparison of observed and standard data from JCPDS card [No.44–1476] show a stannite phase of CFTS in tetragonal space group I-42m, with main diffraction peaks at 2θ value of; 18.25°, 28.25°, 32.85°, 33.37°, 37.83°, 47.51°, and 55.99° corresponding (101) (112), (200), (004), (211), (204), and (312) planes respectively. These results match well with literature [18,20,25,31]. XRD analysis shows no other impurity peaks, (CuS, FeS, SnS), indicating formation of stannite phase of CFTS. Fig. 3 also shows the major peaks of possible impurities Cu_2S [JCPDS card No. 84–1770], FeS [JCPDS card No. 80–1029], and SnS_2 [JCPDS card No. 83–1707]. It is witnessed that CFTS film deposited at 175 °C is amorphous with few

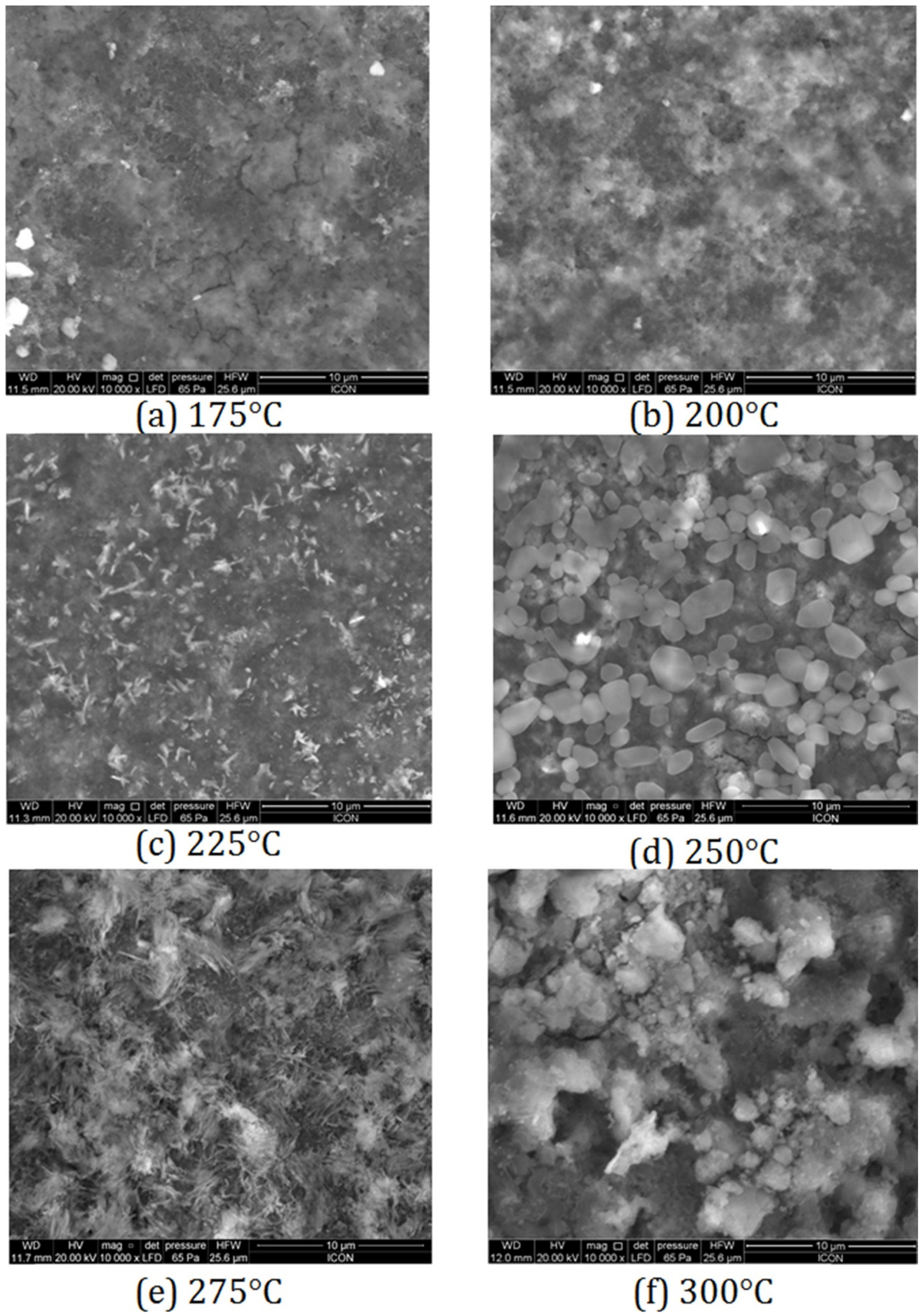

Fig. 5. SEM pictures of CFTS thin films spray deposited at (a) 175 °C, (b) 200 °C, (c) 225 °C, (d) 250 °C, (e) 275 °C, and (f) 300 °C respectively.

peaks of very low intensity consistent to the stannite phase. When deposition temperature rises, the amorphous background weakened and the intensity of the diffraction peaks enriched, this performance is owing to the fact that at low deposition temperature the starting materials ($Cu(NO_3)_2{\cdot}3H_2O$, $FeSO_4{\cdot}7H_2O$, $SnCl_4{\cdot}5H_2O$, and CH_4N_2S) and undesired by-products are present in the films, signifying that the deposition temperature is not adequate for finishing the chemical reaction. CFTS films prepared at and above 200 °C have polycrystalline structure. The lattice parameters are estimated using the relation [24],

$$\frac{1}{d_{hkl}^2} = \frac{h^2 + k^2}{a^2} + \frac{l^2}{c^2} \tag{2}$$

where d is interplanar spacing and (hkl) are the miller indices. The average lattice parameters are estimated to be a = b = 5.53 Å and c = 10.68 Å respectively, which are in close agreement with standard JCPDS values a = b = 5.54 Å and c = 10.73 Å. The shifts in peak position have been perceived with deposition temperature. The peak shifting to lower angles is associated to the increased lattice spacing with decreased deposition temperature.

Crystalline size was estimated by using well known Scherrer's formula [32,33],

$$D = \frac{k\lambda}{\beta cos\theta} \tag{3}$$

where symbols have their usual meaning. The variation of crystalline size with deposition temperature for CFTS thin films is shown in Fig. 4. It is witnessed that crystalline size upsurges with rise in deposition temperature reaches 18 nm at 250 °C and declines thereafter with further increase in deposition temperatures. The obtained values of thicknesses, 2θ, lattice parameters and crystalline size of CFTS thin films are given in Table 1.

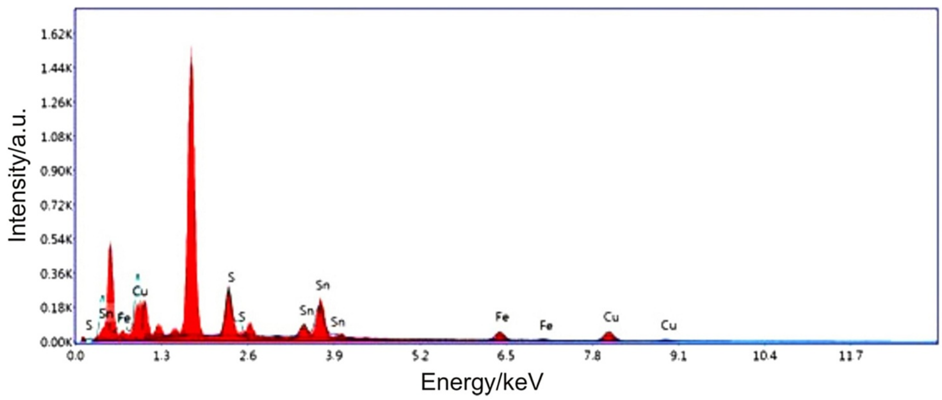

(a) 175°C

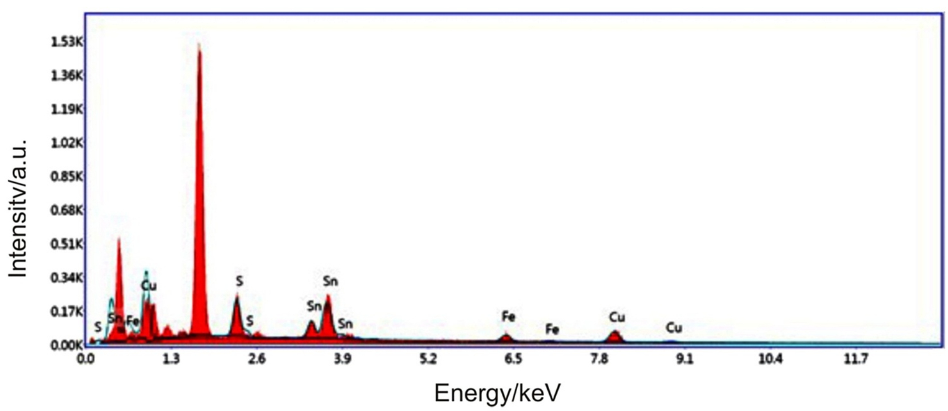

(b) 200°C

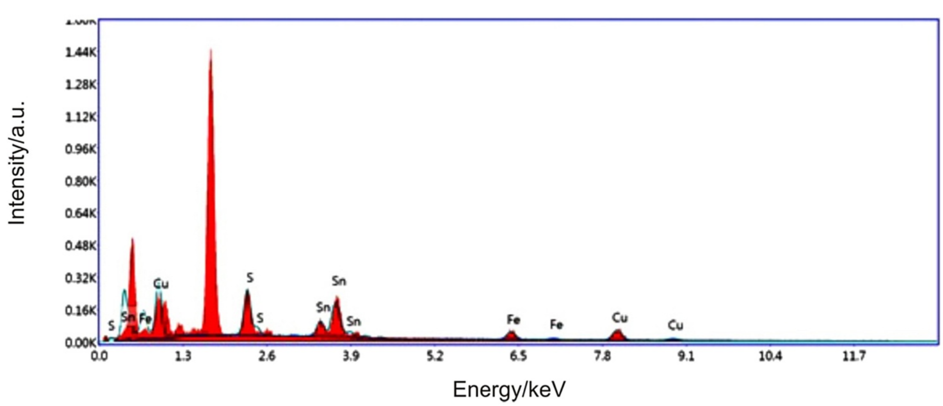

(c) 225°C

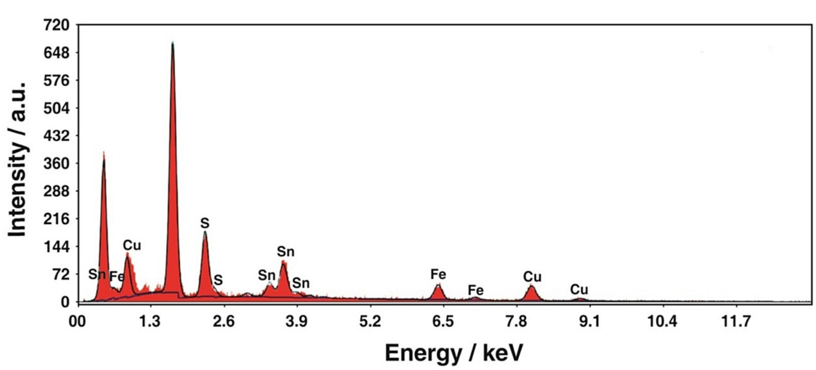

(d) 250°C

Fig. 6. EDAX patterns of CFTS thin films spray deposited at (a) 175 °C, (b) 200 °C, (c) 225 °C, (d) 250 °C, (e) 275 °C, (f) 300 °C and (g) 325 °C respectively.

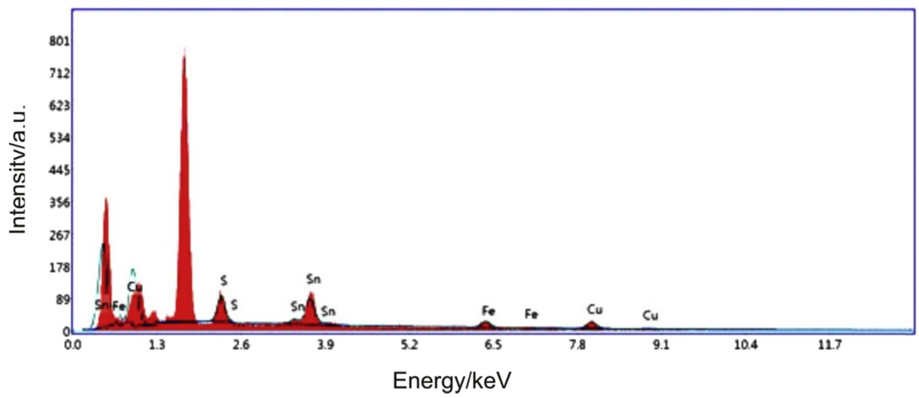

(e) 275°C

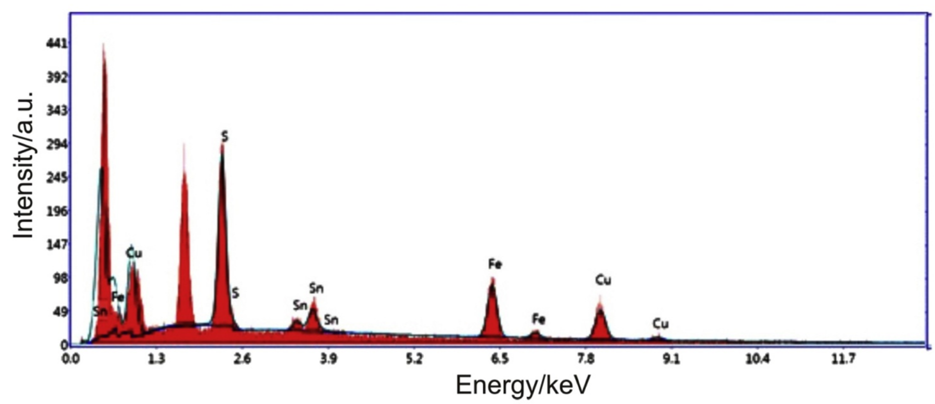

(f) 300°C

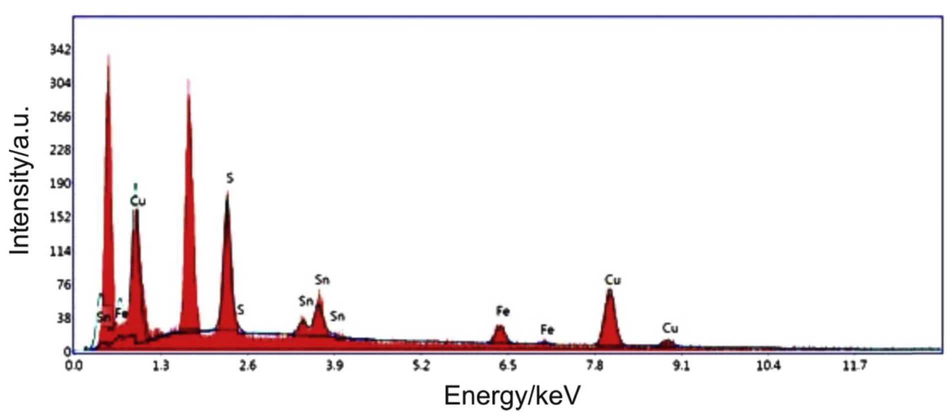

(g) 325°C

Fig. 6. (*continued*)

3.3. Morphological and compositional studies

Fig. 5 shows the SEM pictures of CFTS thin films deposited at various deposition temperatures and 10,000 × magnifications. The CFTS film deposited at 250 °C show uniform and monodisperse particles with hexagonal and double hexagonal pyramid type morphologies. Simillar hexagonal type morphology has been witnessed for solvothermal synthesized of $Cu_2Zn_{1\text{-}x}Fe_xSnS_4$ thin films [34].

EDAX patterns of CFTS thin films spray deposited at various deposition temperatures are shown in Fig. 6. Table 2 shows the atomic percentages in CFTS films deposited at various deposition temperatures from 175 °C to 325 °C. EDAX spectrum indicated peaks corresponding to Cu, Fe, Sn and S, approving the phase and purity of CFTS. EDAX analysis illustrates that atomic ratios of Cu, Fe, Sn and S in CFTS thin film are closer to 2:1:1:4 indicating stoichiometric deposition of CFTS thin films at 250 °C. Above 250 °C, the sulphur deficiency in CFTS films increases with the deposition temperature; this effect could be documented with the copper rich CFTS phases developed during the deposition [35].

3.4. Optical studies

Optical absorption spectra of CFTS thin films deposited at various temperatures were measured in the wavelength range 350–950 nm. In visible region CFTS films have a high coefficient of absorption ($10^4\ cm^{-1}$),

Table 2
Compositional analysis of spray deposited of CFTS thin films.

Deposition Temperature (°C)	Atomic percentage in film by EDAX analysis (%)			
	Cu	Fe	Sn	S
Solution	25.0	12.5	12.5	50.0
175	25	12.2	11.4	51.4
200	25.1	12.4	12	50.5
225	25.1	12.6	12.1	50.2
250	25.9	12.4	12.4	49.3
275	26	12.5	12.3	49.2
300	26.1	12.6	12.4	48.9
325	26	12.5	13	48.5

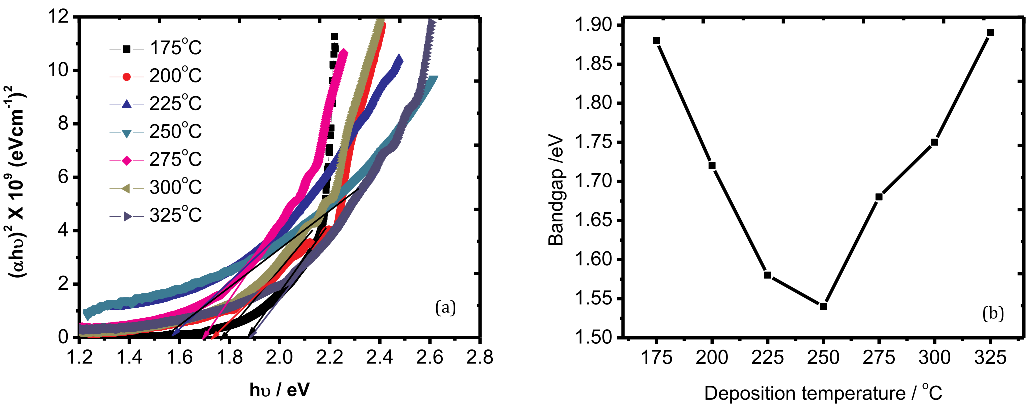

Fig. 7. (a) Variation of $(\alpha h\upsilon)^2$ vs. hυ for CFTS thin films spray deposited at various deposition temperatures. (b) Variation of bandgap with deposition temperature for spray deposited CFTS thin films.

Table 3
Optical and electrical parameters of spray deposited of CFTS thin films. (L.T. - low temperature; H.T. - high temperature).

Deposition Temperature (°C)	Bandgap Eg (eV)	Room temperature Electrical resistivity (× 10^5 Ωcm)	Activation energy (eV) H.T.	L.T.
175	1.88	24.00	0.33	0.09
200	1.72	6.03	0.37	0.10
225	1.58	1.26	0.32	0.10
250	1.54	0.64	0.31	0.12
275	1.68	3.16	0.37	0.13
300	1.75	1.23	0.33	0.10
325	1.89	5.13	0.35	0.08

signifying it's suitability for thin-film solar cell applications. Fig. 7a shows the Tauc's plots $(\alpha h\upsilon)^2$ versus hυ for CFTS thin films. The nature of Tauc's plots suggest direct bandgap for CFTS thin films [36,37]. Fig. 7b shows variation of bandgap with deposition temperature for spray deposited CFTS films. From figure it is witnessed that the bandgap decreases with rise in deposition temperature, becomes minimum (1.54 eV) at 250 °C and upsurges thereafter for further increase in deposition temperature. Above 250 °C, it is perceived that the bandgap marginally upsurges with the rise in deposition temperature. This marginal shift in the bandgap with the rise in deposition temperature is mostly correlated to the increased carrier density. Simillar deposition temperature dependent behavior was previously reported by Bilgin et al. [38] for CdS films. The obtained energy band gaps are 1.88 eV, 1.72 eV, 1.58 eV, 1.54 eV, 1.68 eV, 1.75 eV, 1.89 eV for substrate temperature of 175 °C, 200 °C, 225 °C, 250 °C, 275 °C, 300 °C, and 325 °C respectively, which are in the ideal bandgap range for absorber material normally used in solar cells. The bandgap of 1.54 eV acquired in present case is comparable with 1.508 eV reported for post sulfurized CFTS thin films by Khadka et al. [39]. The bandgap values for CFTS films are given in Table 3.

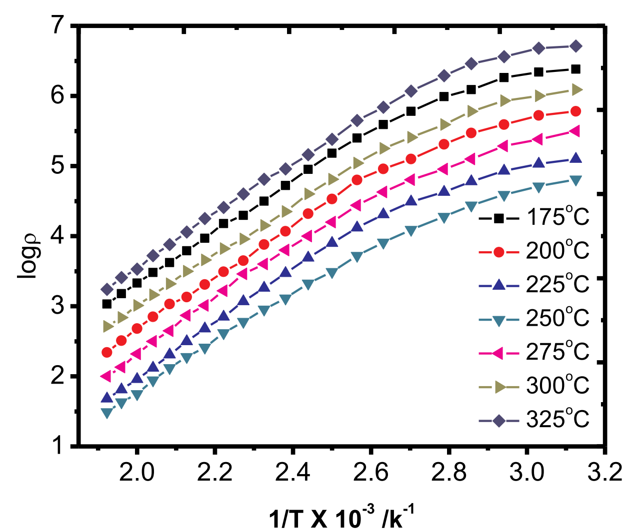

Fig. 8. Variation of logρ vs. with inverse of absolute temperature for spray deposited CFTS thin films.

3.5. Electrical studies

The variations of logρ versus inverse of absolute temperature (1000/T) for CFTS thin films are shown in Fig. 8. It is found that this resistivity variation obeys the Arrhenius equation [40] and the resistivity shrinkages with rise in temperature, demonstrating typical semiconducting performance. It is witnessed that room temperature electrical resistivity shrinkages firstly with upsurge in deposition temperature, becomes lowest (0.646 × 10^5 Ωcm) at 250 °C, and then increases with further upsurge in the deposition temperature. Activation energies are calculated from the slopes of the logρ against inverse of absolute temperature (1000/T) graph. The activation energies are 0.08–0.13 eV and

0.31–0.37 eV in low and high temperature zones respectively. The activation energies confirm that the conduction mechanism in the high- and low-temperature zones is a thermally activated process recognized as thermionic emission and variable range hopping mechanism, respectively [41]. Table 3 presents electrical parameters of the CFTS films deposited at various deposition temperatures.

4. Conclusions

1. The quaternary CFTS thin films are successfully spray deposited on preheated glass substrates at various deposition temperatures (175°C–325 °C).
2. The crystalline sizes are computed and their dependency on deposition temperature has been inspected.
3. The SEM images show uniform and monodisperse particles with hexagonal and double hexagonal pyramid morphologies. EDAX studies confirmed nearly stoichiometric CFTS films.
4. The optical bandgap of 1.54 eV obtained for film deposited at 250 °C, indicates that CFTS films are well suited for thin film solar cell applications.
5. Electrical resistivity study shows semiconducting performance of CFTS thin films.

References

[1] Huafei Guo, Yan Li, Xiaohai Guo, Ningyi Yuan, Jianning Ding, Effect of silicon doping on electrical and optical properties of stoichiometric Cu_2ZnSnS_4 solar cells, Physica B 531 (2018) 9–15.
[2] Juguang Hu, Huo Xiao, Guangxing Liang, Zhenghua Su, Ping Fan, Xiaodong Lin, Preparation of low roughness CZTS thin film and solar cell by SMPLD method, J. Alloy. Compd. 765 (2018) 888–893.
[3] Harun Güney, Demet İskenderoğlu, The effect of Zn doping on CdO thin films grown by SILAR method at room temperature, Physica B 552 (2019) 119–123.
[4] S. Thiruvenkadam, S. Prabhakaran, Sujay Chakravarty, V. Ganesan, Vasant Sathe, M.C. Santhosh Kumar, A. Leo Rajesh, Effect of Zn/Sn molar ratio on the microstructural and optical properties of $Cu_2Zn_{1-x}Sn_xS_4$ thin films prepared by spray pyrolysis technique, Physica B 533 (2018) 22–27.
[5] Mpilo Wiseman Dlamini, Genene Tessema Mola, Near-field enhanced performance of organic photovoltaic cells, Physica B 552 (2019) 78–83.
[6] Seiki Teraji, Jakapan Chantana, Taichi Watanabe, Takashi Minemoto, Development of flexible Cd-free Cu(In,Ga)Se_2 solar cell on stainless steel substrate through multilayer precursor method, J. Alloy. Compd. 756 (2018) 111–116.
[7] Birendra Kumar Rajwar, Shailendra Kumar Sharma, Structural and optical properties of Cu_2ZnSnS_4 synthesized by ultrasonic assisted sol-gel method, Physica B 537 (2018) 111–115.
[8] Shuo Wang, Ruixin Ma, Chengyan Wang, Shina Li, Hua Wang, Incorporation of Rb cations into Cu_2FeSnS_4 thin films improves structure and morphology, Mater. Lett. 202 (2017) 36–38.
[9] Yu P. Gnatenko, P.M. Bukivskij, A.P. Bukivskii, M.S. Furier, Effect of Dy-doping on photoluminescence properties of CdTe crystals and their defect structure, Physica B 546 (2018) 89–92.
[10] Zamaswazi P. Tshabalala, David E. Motaung, Hendrik C. Swart, Structural transformation and enhanced gas sensing characteristics of TiO2 nanostructures induced by annealing, Physica B 535 (2018) 227–231.
[11] T. Feurer, P. Reinhard, E. Avancini, B. Bissig, J. Löckinger, P. Fuchs, R. Carron, T.P. Weiss, J. Perrenoud, S. Stutterheim, S. Buecheler, A.N. Tiwari, Progress in thin film CIGS photovoltaics – research and development, manufacturing, and applications, Prog. Photovoltaics Res. Appl. 25 (2017) 645–667.
[12] Xiaohui Miao, Ruizhi Chen, Wenjuan Cheng, Synthesis and characterization of Cu_2FeSnS_4 thin films prepared by electrochemical deposition, Mater. Lett. 193 (2017) 183–186.
[13] S.A. Vanalakar, P.S. Patil, J.H. Kim, Recent advances in synthesis of Cu_2FeSnS_4 materials for solar cell applications: a review, Sol. Energy Mater. Sol. Cell. 182 (2018) 204–219.
[14] S.A. Vanalakar, S.M. Patil, V.L. Patil, S.A. Vhanalkar, P.S. Patil, J.H. Kim, Simplistic eco-friendly preparation of nanostructured Cu_2FeSnS_4 powder for solar photocatalytic degradation, Mater. Sci. Eng. B 229 (2018) 135–143.
[15] G. El Fidha, N. Bitri, S. Mahjoubi, M. Abaab, I. Ly, Effect of the spraying temperatures and the sulfurization on the properties of the absorber Cu_2FeSnS_4 thin films in a solar cell, Mater. Lett. 215 (2018) 62–64.
[16] Xiankuan Meng, Hongmei Deng, Qiao Zhang, Lin Sun, Pingxiong Yang, Junhao Chu, Investigate the growth mechanism of Cu_2FeSnS_4 thin films by sulfurization of metallic precursor, Mater. Lett. 186 (2017) 138–141.
[17] Xiaoyan Zhang, Ningzhong Bao, Karthik Ramasamy, Yu-Hsiang A. Wang, Yifeng Wang, Baoping Lin, Arunava Gupta, Crystal phase-controlled synthesis of Cu_2FeSnS_4 nanocrystals with a band gap of around 1.5 eV, Chem. Commun. 48 (2012) 4956–4958.
[18] Hao Guan, Honglie Shen, Baoxiang Jiao, Xu Wang, Structural and optical properties of Cu_2FeSnS_4 thin film synthesized via a simple chemical method, Mater. Sci. Semicond. Process. 25 (2014) 159–162.
[19] Chao Dong, Getinet Y. Ashebir, Juanjuan Qi, Junwei Chen, Mingtai Wang, Solution-processed Cu_2FeSnS_4 thin films for photovoltaic application, Mater. Lett. 214 (2018) 287–289.
[20] Xing Jiang, Wei Xu, Ruiqin Tan, Weijie Song, Jianmin Chen, Solvothermal synthesis of highly crystallized quaternary chalcogenide Cu_2FeSnS_4 particles, Mater. Lett. 102–103 (2013) 39–42.
[21] Krishnaiah Mokurala, Parag Bhargava, Sudhanshu Mallick, Single step synthesis of chalcogenide nanoparticles Cu_2ZnSnS_4, Cu_2FeSnS_4 by thermal decomposition of metal precursors, Mater. Chem. Phys. 147 (2014) 371–374.
[22] Faruk Ozel, Mahmut Kus, Adem Yar, Emre Arkan, Mustafa Can, Abdalaziz Aljabour, Nurhan Mehmet Varal, Mustafa Ersoz, Fabrication of quaternary Cu_2FeSnS_4 (CFTS) nanocrystalline fibers through electrospinning technique, J. Mater. Sci. 50 (2015) 777–783.
[23] R.R. Prabhakar, N. HuuLoc, M.H. Kumar, Pablo P. Boix, Juan Sun, R.A. John, SudipK. Batabyal, L.H. Wong, Facile water-based spray pyrolysis of earth abundant Cu_2FeSnS_4 thin films as an efficient counter electrode in dye-sensitized solar cells, ACS Appl. Mater. Interfaces 6 (2014) 17661–17667.
[24] D.B. Khadka, JunHo Kim, Structural, optical and electrical properties of Cu_2FeSnX_4(X= S, Se) thin films prepared by chemical spray pyrolysis, J. Alloy. Compd. 638 (2015) 103–108.
[25] Yan Chang, Chun Huang, Yang Jia, Fangyang Liu, Jin Liu, Yanqing Lai, Jie Li, Yexiang Liu, Synthesis and characterizations of quaternary Cu_2FeSnS_4 nanocrystals, Chem. Commun. 48 (2012) 2603–2605.
[26] Xiankuan Meng, Huiyi Cao, Hongmei Deng, Wenliang Zhou, Jiahua Tao, Lin Sun, Fangyu Yue, Pingxiong Yang, Junhao Chu, Synthesis and characterization of Cu-based selenide photovoltaic materials: Cu_2FeSnS_4 and Cu(In,Al)Se_2, J. Alloy. Compd. 644 (2015) 354–362.
[27] A.A. Yadav, M.A. Barote, P.M. Dongre, E.U. Masumdar, Studies on growth and characterization of $CdS_{1-x}Se_x$ ($0.0 \le x \le 1.0$) alloy thin films by spray pyrolysis, J. Alloy. Compd. 493 (2010) 179–185.
[28] Guilin Chen, Jianmin Li, Shuiyuan Chen, Zhigao Huang, Miaoju Wu, Jifu Zhao, Weihuang Wang, Haiqin Lin, Changfei Zhu, Low cost oxide-based deposition of Cu_2FeSnS_4 thin films for photovoltaic absorbers, Mater. Chem. Phys. 188 (2017) 95–99.
[29] L. Kasturi, Chopra, Thin Film Phenomena, McGraw-Hill, New York, 1969.
[30] A.A. Yadav, S.D. Salunke, Properties of spray deposited nanocrystalline indium selenide thin films, J. Mater. Sci. Mater. Electron. 26 (2015) 5416–5425.
[31] Jicheng Zhou, Zhibin Ye, Yunyun Wang, Qiang Yi, Jiawei Wen, Solar cell material Cu_2FeSnS_4 nanoparticles synthesized via a facile liquid reflux method, Mater. Lett. 140 (2015) 119–122.
[32] P. Scherrer, Bestimmung der Größe und der inneren Struktur von Kolloidteilchen mittels Röntgenstrahlen, Göttinger Nachrichten Gesell. 2 (1918) 98.
[33] A. Patterson, The Scherrer formula for X-ray particle size determination, Phys. Rev. 56 (1939) 978–982.
[34] Zohreh Shadrokh, Yazdani Ahmad, Hosein Eshghi, Solvothermal synthesis of $Cu_2Zn_{1-x}Fe_xSnS_4$ nanoparticles and the influence of annealing conditions on drop-casted thin films, Semicond. Sci. Technol. 31 (2016) 045004.
[35] Mazabalo Baneto, Alexandru Enesca, Ciprian Mihoreanu, Yendoubé Lare, Koffi Jondo, Kossi Napo, Anca Duta, Effects of the growth temperature on the properties of spray deposited $CuInS_2$ thin films for photovoltaic applications, Ceram. Int. 41 (2015) 4742–4749.
[36] X.L. Tong, D.S. Jiang, W.B. Hu, Z.M. Liu, M.Z. Luo, The comparison between CdS thin films grown on Si(111) substrate and quartz substrate by femtosecond pulsed laser deposition, Appl. Phys. A 84 (2006) 143–148.
[37] Xiankuan Meng, Hongmei Deng, Jiahua Tao, Huiyi Cao, Xinran Li, Lin Sun, Pingxiong Yang, Junhao Chu, Heating rate tuning in structure, morphology and electricity properties of Cu_2FeSnS_4 thin films prepared by sulfurization of metallic precursors, J. Alloy. Compd. 680 (2016) 446–451.
[38] V. Bilgin, S. Kose, F. Atay, I. Akyuz, The effect of substrate temperature on the structural and some physical properties of ultrasonically sprayed CdS films, Mater. Chem. Phys. 94 (2005) 103–108.
[39] D.B. Khadka, JunHo Kim, Structural transition and band Gap tuning of Cu_2(Zn,Fe) SnS_4 chalcogenide for photovoltaic application, J. Phys. Chem. C 118 (2014) 14227–14237.
[40] A.S. Hassanien, Alaa A. Akl, Effect of Se addition on optical and electrical properties of chalcogenide CdSSe thin films, Superlattice. Microst. 89 (2016) 153–169.
[41] Abdelhalim M. Ziqan, A.F. Qasrawi, Abdulftah H. Mohammad, N.M. Gasanly, Thermally assisted variable range hopping in Tl4S3Se crystal, Bull. Mater. Sci. 38 (2015) 593–598.